THE JOURNAL OF COMPARATIVE NEUROLOGY 495:709–721 (2006)

Synaptic Connection from Cortical Area V4 to V2 in Macaque Monkey

JOHN C. ANDERSON* AND KEVAN A.C. MARTIN*
Institute for Neuroinformatics, University of Zürich, and ETH Zürich, 8057 Zürich, Switzerland

ABSTRACT

The major target of the V4 projection in V2 is layer 1, where it forms a tangential spread of asymmetric (excitatory) synapses. This is characteristic of a "feedback" projection. Some axons formed discrete clusters of bouton terminaux between lengths of myelinated axon, while others were unbranched and formed a continuous distribution of en passant boutons with no intercalated myelin. Minor projections were found in layers 2/3 and 6. Dendritic spines were the most frequently encountered targets of the V4 projection (80% in layer 1 and layer 2/3, 94% in layer 6). The remaining targets were dendritic shafts. In layer 1, 69% of target dendrites (12% of all targets) had characteristics identifying them as smooth (GABAergic) cells. In layer 2/3 and layer 6 virtually all the shaft synapses were on smooth dendrites (86% and 100%, respectively). Multisynaptic boutons were rare (mean 1.1 synapses per bouton). Synapses formed in layer 6 were smaller than those of layer 1 (mean area 0.073 μm^2 vs. 0.117 μm^2). Synapses formed with spines had a more complex postsynaptic density than those formed with dendritic shafts. With respect to targets and synaptic type and size and morphology of synapses, the feedback projection from V4 to V2 resembles those of feedforward projections. The principal difference between the feedforward and feedback projection is in the lamina location of their terminal boutons. The concentration of the V4 projection on layer 1, where it forms asymmetric synapses mainly with spines, suggests that it excites the distal apical dendrites of pyramidal cells. J. Comp. Neurol. 495:709–721, 2006.

Indexing terms: visual cortex; area V2; corticocortical; light and electron microscopy; synapse morphology; postsynaptic target

The existence of "feedback" cortical projections that are thought to perform "top-down" operations has long been known. Although these projections are a crucial part of the interpretation of behavioral and physiological studies, surprisingly little is known of the details of these projections. In the primate cortex such projections have been defined mainly on the basis of their pattern of termination in the different laminae of the target cortical area. Unlike "feedforward" projections, whose canonical pattern is to terminate principally in layer 4, the feedback projections terminate outside layer 4, with layer 1 being a prominent target. These projections have been studied mainly at the light microscope level and much of what we know about the details of individual axonal arborizations comes from the extensive reconstructions of feedback and feedforward projections made by Rockland and colleagues (reviewed in Rockland, 1994, 1997). Their reconstructions of the feedback axons from V4 to V2 indicate that layers 1, 2, and 6 are the preferred layers of innervation and this laminar organization seems to be a cardinal feature of the feedback projections seen at the single fiber level. An additional feature of the feedback projection noted in a number of studies is that they are more divergent, spreading over a wider territory than the feedforward projections (Krubitzer and Kaas, 1989; Shipp and Zeki, 1989a,b; Suzuki et al., 2000; Stettler at al., 2002). The studies of Rockland at the single fiber level also indicate such divergence in the feedback connections, including those from V4 to V2

Grant sponsor: European Union; Grant number: QULG3-1999-01064 (to K.A.C.M.); Grant sponsor: Human Frontier Science Program; Grant number RG0123/2000-B (to K.A.C.M.).

*Correspondence to: John C. Anderson or Kevan A.C. Martin, Institute for Neuroinformatics, University of Zürich and ETH Zürich, Winterthurerstr.190, 8057 Zürich, Switzerland.
E-mail: jca@ini.phys.ethz.ch or kevan@ini.phys.ethz.ch

Received 2 August 2005; Revised 5 October 2005; Accepted 11 November 2005

DOI 10.1002/cne.20914

Published online in Wiley InterScience (www.interscience.wiley.com).

(Rockland et al., 1994). Presumably these features reflect basic differences in the functional role of the two types of intracortical projection.

The projection from V2 to V4 has been extensively studied because it is part of the fan-out from early visual areas to the dorsal and ventral processing streams. Staining V2 with the mitochondrial enzyme cytochrome oxidase provided evidence for stripe-shaped compartments within V2 (Livingstone and Hubel, 1982), which reflect differences in the input from V1 (Sincich and Horton, 2005) and the output projections from V2 to anterior visual areas. Thick and thin stripes alternate and are separated by paler staining interstripes. The thick stripes project mainly to area V3 and V5, while the thin stripes and interstripes project to V4 (Shipp and Zeki, 1985, 1989a,b; De Yoe and Van Essen, 1985). Interestingly, the visual latencies of neurons in V2 are closely correlated with their position with the stripes (Munk et al., 1995). Neurons in thick and pale stripes respond on average 20 ms before those in the thin stripes.

The projection from V4 to V2 is far less well studied and there are no studies at the ultrastructural level. Here we studied the projection of individual axons and groups of axons at the light (LM) and electron (EM) microscope level. Our motivation was to gather at the ultrastructural level clues as to the differences between the feedforward projections we have studied previously and the feedback projections. By taking a classic feedback pathway, we could describe quantitatively the synaptic organization and so provide a direct comparison of feedforward projections. This study shows that with respect to their target neurons, and the size and density of synapses, the V4 to V2 projection is similar to the feedforward projections from V1 to MT, V2 to V3A, and V2 to MT. Unlike the feedforward projections, the feedback projection seldom forms patches in its terminal layers. Its concentration in layer 1 suggests that it connects principally to the distal apical dendrites of pyramidal cells.

MATERIALS AND METHODS

The material presented here was taken from two adult male macaque monkeys (*Macaca mulatta*). Animal treatment and surgical protocols were carried out in accordance with the guidelines of the Kantonal Veterinaeramt of Zurich. The following procedures are similar to those used in Anderson and Martin (2002). Animals were prepared for surgery after the administration of an intramuscular premedication of xylazine (Rompun, Beyelar, 0.5 mg/kg)/ketamine (Ketalar, Parke Davis, 10 mg/kg). This was followed by cannulation of a femoral vein for the delivery of alphaxalone/alphadalone (Saffan, Glaxo) to establish complete anesthesia.

Each animal received ionophoresed injections of the neuronal tracer biotinylated dextran amine (BDA) (Molecular Probes, Eugene, OR). One animal received four injections of 10% BDA in 0.01 M phosphate-buffered saline, pH 7.4 (PBS). The second animal received seven injections. The BDA was delivered from a glass micropipette using a pulsed ionophoretic current of 2–4 mA over a 7–10-minute period. After a 14-day survival period the animals were very deeply anesthetized with intravenous (i.v.) pentobarbital (20 mg/kg) and then perfused transcardially with a normal saline solution, followed by a solution of 3.5% paraformaldehyde, 0.8% glutaraldehyde, and 15% picric acid in 0.1 M PB, pH 7.4. The brain was removed from the skull and a block of cortex containing the injection site and areas V1/V2 was removed. The block was allowed to sink in sucrose solutions of 10, 20, and 30% in 0.1 M PB, then freeze-thawed in liquid nitrogen and washed in 0.1 M PB. Sections were cut from the block at 80 μm in the parasagittal plane and collected in 0.1 M PB. We used standard procedures to reveal the neuronal tracers. In brief outline, washes in PBS were followed by 10% normal swine serum (NSS) in PBS (1 hour). Further washes in NSS preceded overnight exposure (5°C) to an avidin-biotin complex (Vector Laboratories, Burlingame, CA; ABC kit, Elite). The peroxidase activity was identified using 3,3-diaminobenzidene tetrahydrochloride (DAB). After assessment by light microscopy, selected regions of tissue were treated with 1% osmium tetroxide in 0.1 M PB. Dehydration through alcohols (1% uranyl acetate in 70% alcohol) and propylene oxide allowed flat mounting in Durcupan (Fluka, Buchs, Switzerland) on glass slides.

Light microscopic observations of labeled axons were carried out to locate and select regions of interest for electron microscopy. We reconstructed individual collaterals in the less densely innervated areas for correlated light and electron microscopy. Serial ultrathin sections were collected at 60 or 70 nm thickness on Pioloform-coated single slot copper grids. Labeled boutons were photographed at a magnification of 21,000. Synapses and associated structures were classified using conventional criteria (Peters et al., 1991). Collections of serial sections were digitized and reconstructed using Trakem, an in-house EM-digitization package. To measure and display the postsynaptic densities of labeled boutons we used software developed by ourselves, described in outline elsewhere (see Materials and Methods; Anderson et al., 1998).

The estimates of labeled bouton density were derived using the physical disector method (Sterio, 1984). We selected regions of particularly dense innervation by labeled axon for reembedding. Serial 70-nm-thick sections were collected from these regions and a "reference" and "look-up" section was selected. The reference and look-up sections were separated by one section. Photographs were taken with the electron microscope to form patches of tissue, e.g., 5×5 images. Five different patches of cortex were photographed in this way, ranging in area from 500–1,070 μm^2. All electron micrographs were taken at 11,500×. Synapses that were in the reference section, but that disappeared in the look-up section, were counted. Synapses that were present in both look-up and reference sections were not counted (Sterio, 1984). Adobe Photoshop CS (San Jose, CA) and Adobe Illustrator CS were used to prepare digital photomicrographs and enhance image contrast.

RESULTS

Light microscopy

Each of two monkeys received ionophoretic injections of BDA into area V4 along the edge of the prelunate gyrus and close to the lunate sulcus (Fig. 1A). Ionophoretic injections were all confined to the gray matter of V4 and BDA label could be seen in all laminae (Fig. 1B) except layers 1 and 2, which made it impossible to identify the precise laminar location of the cells of origin of the projection to V2. In both animals the injections were made into

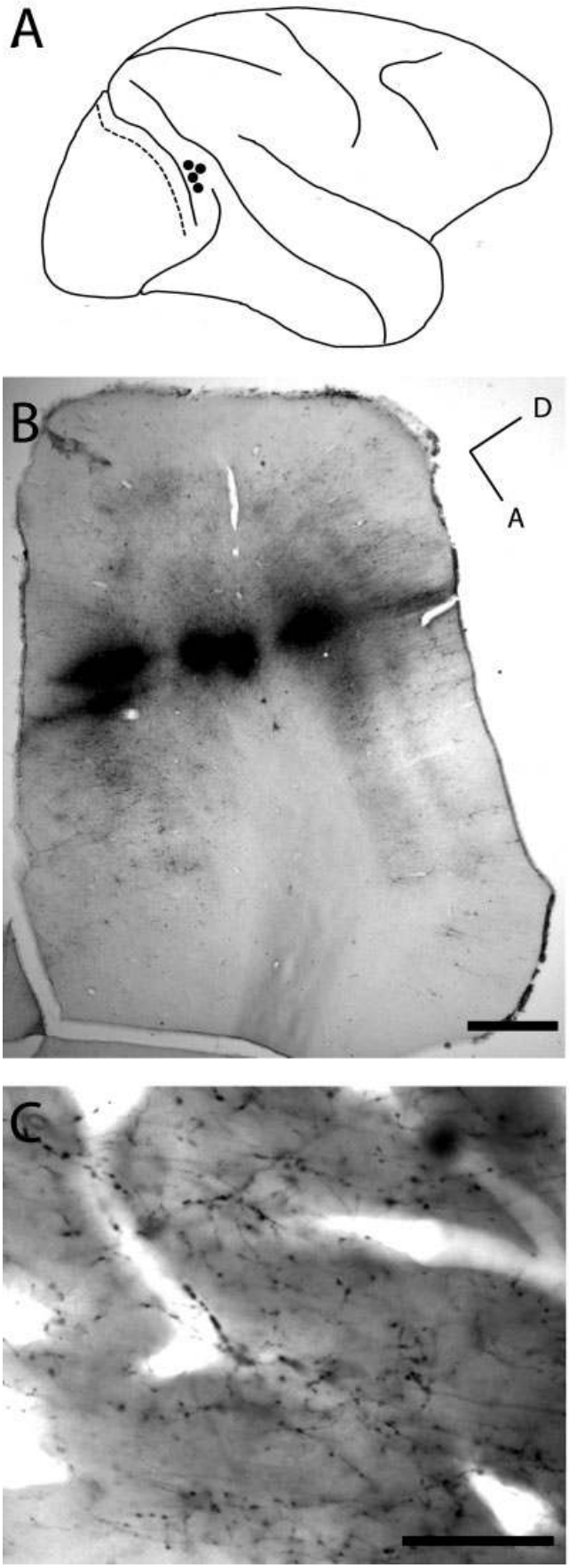

the dorsal surface of V4; approaching from directly above the gyrus and passing through cortex to run parallel with the laminae in the anterior bank of the sulcus, or from a more lateral position and passing through the thickness of cortex. In the latter case one ionophoretic site was very close to the white matter (Fig. 1B), although the label was taken up by layer 6 neurons and a few cells in the white matter. BDA labeling was excellent at the injection site. In one animal the labeling was densest at the site of ionophoresis (Fig. 1B). In the second animal the labeling was densest in a halo of processes around the site of ionophoresis. Most of the uptake was by pyramidal cells of layers 2/3, 5, and 6.

Myelin on axons provides a barrier to the penetration of the reagents and thus were not stained other than at their cut ends, nodes, or where the beaded collaterals emerged. However, because the osmium staining enhanced the contrast of the myelinated fibers, they could be followed through the neuropil.

Anterograde labeling was seen in extrastriate visual areas along with some pale-stained somata deep in layer 6 and occasionally layer 3 of the superior temporal sulcus. In one animal the strongest anterograde transport was to V2 where the fibers entered from the white matter and, with minor branchlets in layer 6, passed directly through all cortical laminae until layer 1, where they divided to produce long rays of aligned fibers that coursed through layer 1 for several millimeters. Most of the fibers appeared to traverse layer 1 toward the tip of the gyrus in the direction of the V1/V2 border, although many had clearly been sectioned, contributing to the puncta-like appearance of the innervation site. The axons showed numerous distinct varicose swellings that proved to be synaptic boutons. Occasionally, collaterals descended from the areas of dense innervation in layer 1 to form additional boutons in layer 2/3. There was also a rather sparse innervation of layer 6 by very fine collaterals, which had tiny varicose swellings. No cell or terminal labeling was evident in other layers. In the second animal, two collaterals passed through layer 1 in V2, where they traversed several millimeters of layer 1, climbing to the tip of the gyrus to almost the V1/V2 border.

The profusion of axons and en passant and terminaux boutons in layer 1 did not present the typically patchy appearance to the innervation characteristic of feedforward projections. Although occasional individual axons did form clusters (Fig. 3B,C), most axons radiated through layer 1 to form an extensive homogenous tangle of processes (e.g., Figs. 1C, 2A, 4A,B). The density of the innervation of layers 2 and 3 fell away rapidly with lateral distance from the main projection zone in layer 1.

Fig. 1. Location of injection sites. **A:** Schematic drawing of a macaque brain showing region in which injections were made (filled circles) in the prelunate gyrus. The border between visual areas V1 and V2 is indicated by a dotted line. **B:** Photomontage of parasagittal section through prelunate gyrus of macaque brain showing five injection sites in area V4. Axes indicate: dorsal (D), anterior (A). **C:** Light micrograph showing labeled axon termination site in layer 1 of V2. Scale bars = 1 mm in B; 25 μm in C.

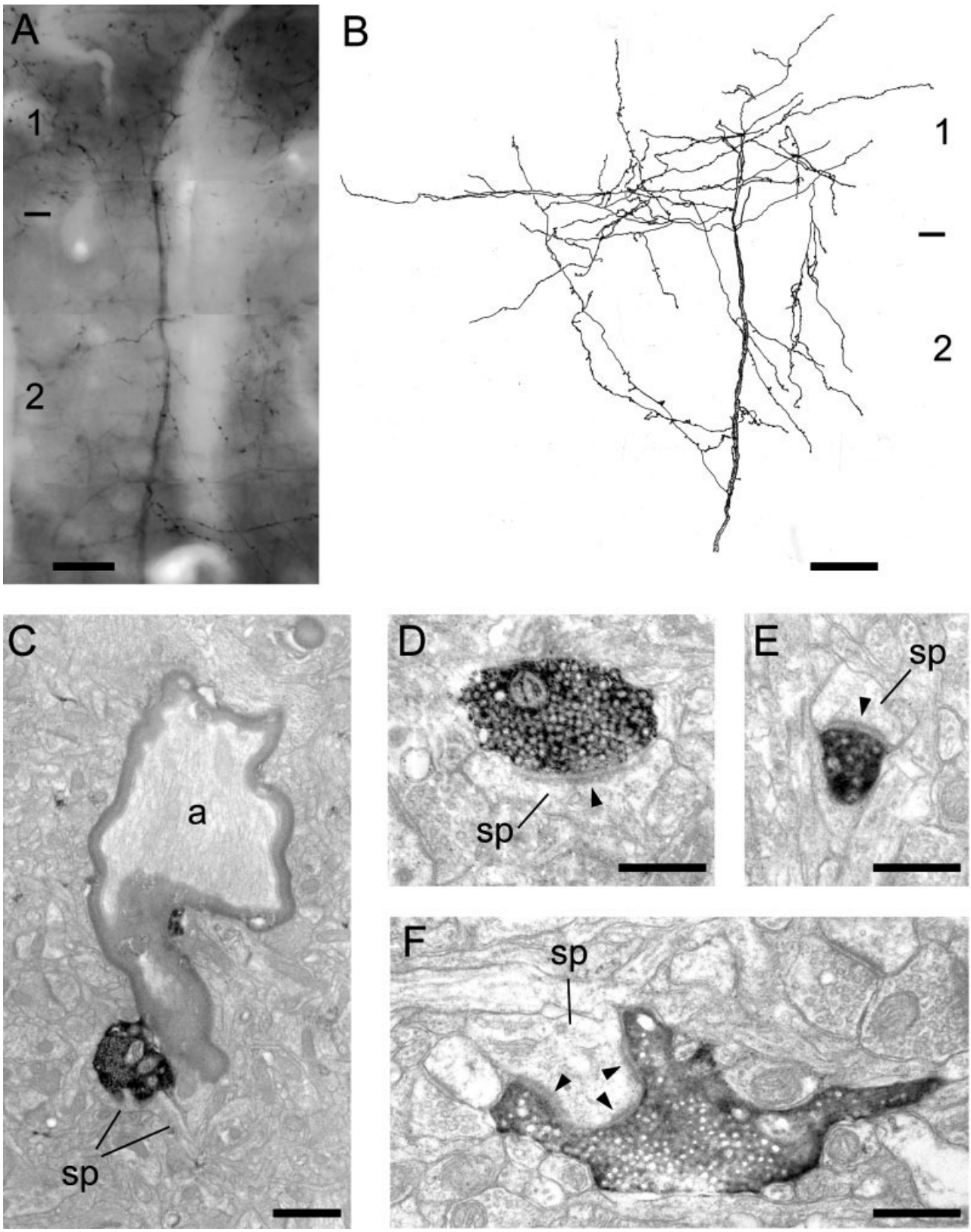

Fig. 2. Light and electron micrographs taken from cortical area V2 showing BDA labeled axons and their terminals. **A:** Labeled terminals form dense band in layer 1 and lesser projections into layer 2/3. A large-caliber labeled axon can be seen rising through the cortex to arborize from an intensely labeled node in layer 1. Laminae and their boundaries are indicated to the left. **B:** Light microscopic reconstruction of large-caliber axon seen in A. The reconstruction is made from a single 80-μm-thick section. Laminae and their boundaries are indicated to the right. **C–F:** Electron photomicrographs of labeled boutons taken from layers 1 and 2 shown in A. C: Low-power picture of large labeled bouton in layer 2 adjacent to the thick parent axon (a) seen in A and B. The bouton forms a synapse with a spine (sp). The axon appears not labeled due to the axon being covered with a myelin sheath. The axon is visible in the LM because the myelin is stained by the osmium. D: A medium-sized labeled bouton in layer 2 forms an asymmetric synapse (solid arrowhead) with a spine (sp). E: A small labeled bouton in layer 2 forms an asymmetric synapse (solid arrowhead) with a small spine (sp). F: A large labeled bouton forms a perforated asymmetric synapse (solid arrowheads) with a spine (sp). Scale bars = 25 μm in A; 50 μm in B; 1 μm in C; 0.5 μm in D–F.

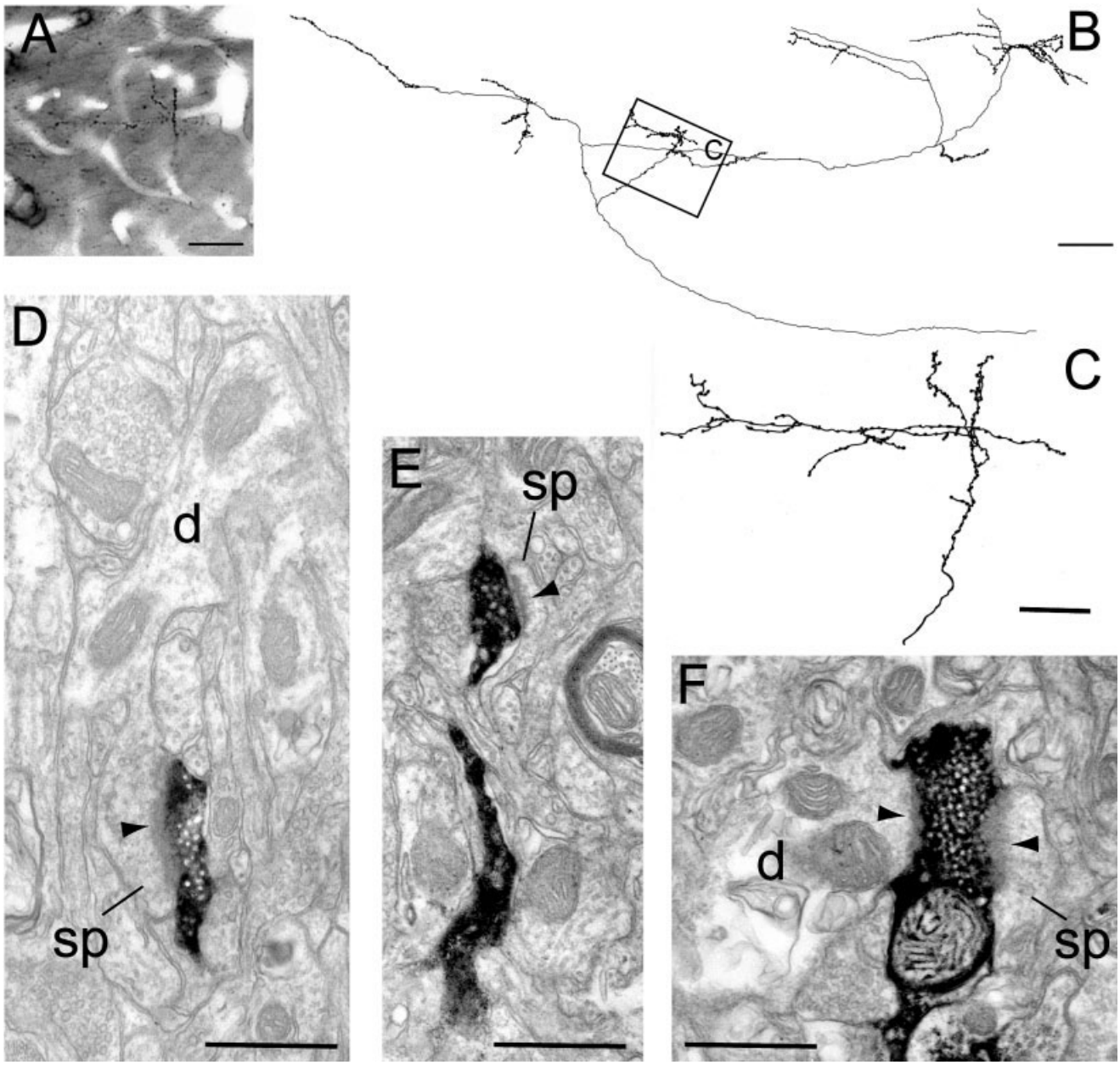

Fig. 3. Light and electron micrographs of BDA-labeled axon and boutons located in layer 1 of area V2. **A:** Photomicrograph showing collateral and varicose swellings of axon in layer 1. **B:** Light microscopic reconstruction of axon (seen in A) forming arbors restricted to layer 1. The box-shaped boundary (C) represents the area shown in the photomicrograph in A and the reconstructed detail shown in C. **C:** A light microscopic reconstruction of a single clustered arbor shown in A and highlighted in the reconstruction in B. The varicose swellings or boutons were restricted to the arbors. **D–F:** Examples of synapses formed with spines and dendrites. D: A labeled bouton forms an asymmetric synapse (solid arrowhead) with a spine (sp) that can be traced back to the parent dendrite (d). E: A small labeled bouton forms an asymmetric synapse (solid arrowhead) with a small spine (sp). F: A labeled bouton forms asymmetric synapses with a spine (sp) and a dendritic shaft (d). Following the dendrite through serial sections showed that it contained numerous mitochondria and formed synapses with unidentified boutons. Such dendrites belong to GABA containing neurons with smooth dendrites. Scale bars = 25 μm in A; 0.1 mm in B; 25 μm in C; 0.5 μm in D–F.

Electron microscopy

We examined a total of 145 boutons, including 90 boutons from layer 1, 27 from layer 2/3, and 28 from layer 6. Of this sample, 136 single boutons were serially sectioned and completely reconstructed so that the area of the synaptic density could be measured. The remaining nine boutons were not sufficiently complete for quantification of their synapses, but were used in the assessment of synaptic targets. All synapses

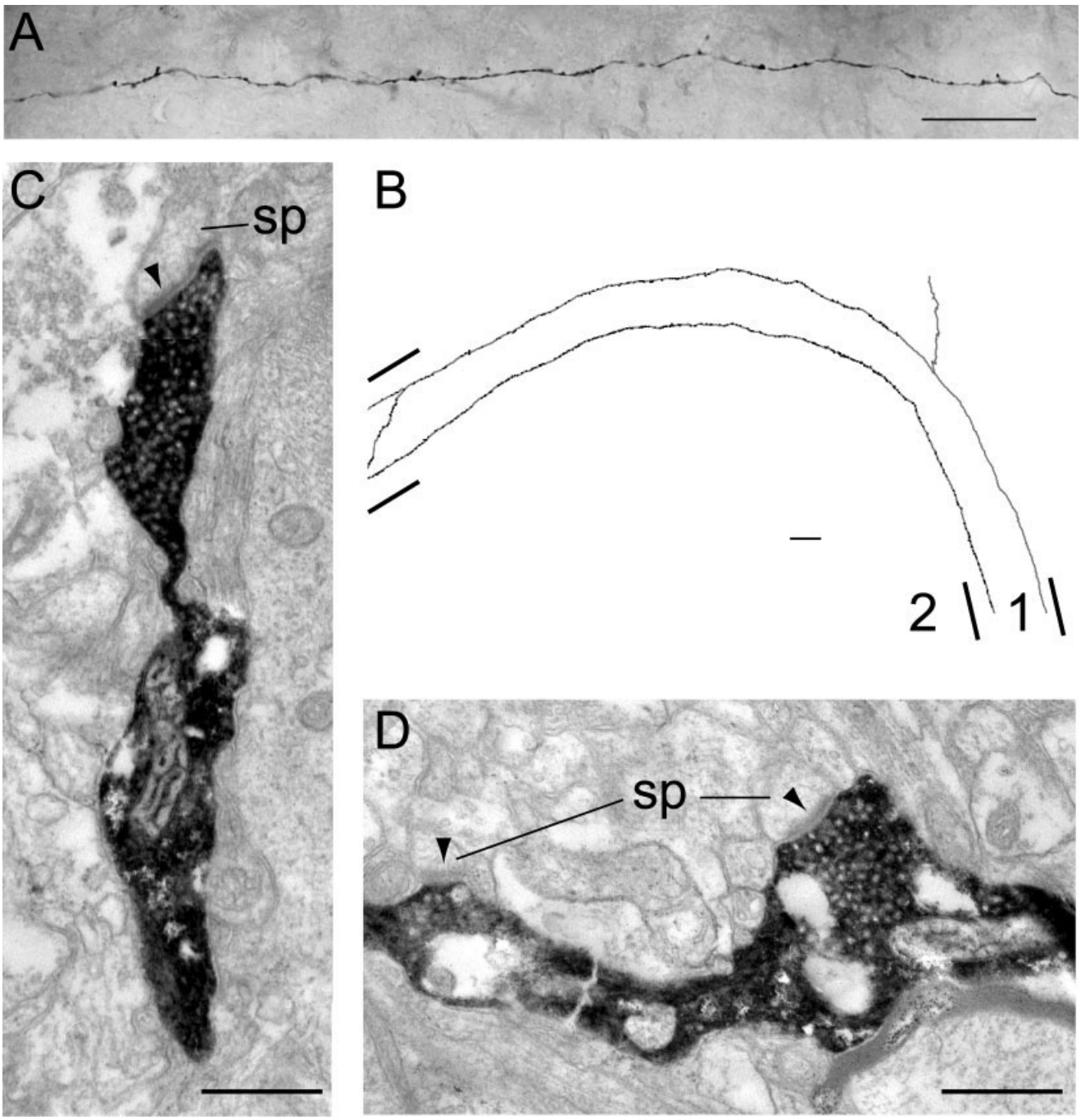

Fig. 4. Light and electron micrographs of BDA-labeled axons and boutons located in layer 1 of area V2. **A:** Photomontage of a labeled collateral taken from layer 1. Numerous varicose swellings of the en passant and aux terminaux types can be seen along the axon length. **B:** Light microscopic reconstruction of collateral shown in A. The axons arise from the right forming very few branches. Laminae and their boundaries are indicated. **C:** Electron micrograph montage of a labeled bouton terminaux taken from the unbranched collateral shown in A. The bouton forms an asymmetric synapse (solid arrow head) with a spine (sp). **D:** Two labeled boutons en passant each forms an asymmetric synapse (solid arrowheads) with a spine (sp). Scale bars = 25 μm in A; 100 μm in B; 0.5 μm in C,D.

formed by labeled boutons were asymmetric (Gray's type 1).

The reaction endproduct was dark, although its intensity varied between boutons. Synaptic vesicles and mitochondria were clearly visible within the boutons and occasional boutons contained vacuoles (Fig. 4C,D). Most boutons were small (<0.5 μm), although the sample showed a considerable range of sizes. The boutons were filled with synaptic vesicles and usually contained at least one mitochondria. Within the target structure there was a

clear postsynaptic density. Puncta adherens (n = 9), when present, were closely associated with a synapse and its postsynaptic target. They could be identified by an absence of presynaptic vesicles within the bouton and a density (similar to the postsynaptic density) within the presynaptic terminal that was mirrored by a density within the target structure (Peters et al., 1991). Puncta were not included in our measurements of synapse size.

Synaptic targets were identified using standard ultrastructural criteria (Peters et al., 1991). Serially sectioning the bouton and its synaptic target assisted greatly in the identification of the target type. The majority of targets were spines (83%), the remainder were dendrites. We reconstructed the complete spine in order to discover if it received a second input, although following the spine neck back to its parent dendrite often proved impossible. Approximately 6% of the reconstructed spines received a second synapse from an unlabeled bouton. The second synapse was always identified as a symmetric (Gray's type 2) synapse. Dendrites often contain mitochondria or microtubules, making identification relatively simple.

Axons and their boutons

We reconstructed three single axons to illustrate the variety of axons seen in this projection (Figs. 2A,B, 3A–C, 4A,B). We sampled boutons from three regions: the densest area of innervation (Figs. 1C, 2A), ~500 μm posterior to this region (Fig. 3), and ~2 mm anterior of the region in which the axons appeared to arrive in layer 1 of V2 (Fig. 4). Axons tended to branch only when they reached layer 1 and not in the deeper layers. Figure 2A,B shows a photomicrograph and a partial reconstruction of an axon arborizing in layer 1. The majority of collaterals radiated away from the main axon trunk and traveled through layer 1. This axon also sent descending collaterals to the middle of layer 2/3 (Fig. 2A,B). The reconstruction is from a single 80-μm-thick section because the arbor was close to the densest region of innervation by labeled axons and so could not be traced unambiguously through adjacent sections. The axon is therefore not completely reconstructed, although it was striking because of the large caliber myelinated axon trunk (>2 μm, Fig. 2C) and the extensively branched collaterals.

Layer 1 boutons taken from this region for EM analysis could not be correlated with our LM observations because of the sheer density of labeled terminals. In sectioning through this dense region, we obtained a random sample of 46 labeled boutons forming 48 synapses. The boutons all came from the area in which we found the reconstructed axon illustrated in Figure 2C. The majority of synapses were formed with spines (75%) (Fig. 2D–F) and the remainder with dendritic shafts.

As well as examining the labeled boutons from this region of layer 1, we also measured the diameter of labeled, unmyelinated axons (n = 50) in the same region. There was remarkably little variation in size, the largest diameter reaching 0.25 μm, with a mean of 0.1 μm (standard error of the mean [SEM] = 0.007 μm).

The boutons in layer 2 (n = 27) could be correlated with our LM observations as there were very few labeled processes in this lamina. A labeled descending axon collateral pursued the same path as the parent ascending afferent axon trunk. In the LM it appeared to be in close apposition with the trunk and this was confirmed in the EM (Fig. 2C). The labeled boutons of layer 2/3 appeared to be somewhat larger (~1 μm, Fig. 2C) than the majority of those seen in layer 1, although this was not always the case (e.g., Fig. 2E). The 27 boutons formed 34 synapses. Boutons forming more than one synapse usually had a larger diameter. Only two of the target spines examined showed a second, symmetric synapse formed by an unlabeled bouton.

Axon 1

Another pattern of innervation by V4 axons in layer 1 can be seen in Figure 3. In this rare example, the bouton-rich axon collaterals formed grape-like clusters of boutons (Fig. 3A). The reconstructed axon shows the clusters separated by lengths of myelinated axon with no en passant boutons between arbors (Fig. 3B). The boutons within the clusters were closely spaced and covered all parts of the collateral (Fig. 3C). Most of the boutons on this axon were en passant: bouton terminaux represented only 18% of the boutons. Most of the boutons (89%) formed synapses with small to medium sized spines (Fig. 3D–F) and seldom with dendrites (Fig. 3F). Only one of the target spines formed a second, symmetric synapse.

Axon 2

The morphology of labeled axons most commonly found in layer 1 had more regular distribution of boutons over extensive lengths (>2 mm) of fine axon collateral (Fig. 4A). Varicose boutons were clearly visible, and because of the straight and largely unbranched trajectory of the collaterals, the bouton terminaux (26% of boutons) were particularly prominent. During the reconstruction of this axon (Fig. 4B) it became evident that the more proximal portions of the axon were myelinated and showed no bouton-like varicosities.

The ultrastructural quality of these axons was inferior to the other material used in this study (Fig. 4C,D). Nevertheless, we examined 22 boutons from these axons. Synapses formed mostly with spines (83%), the majority of which were rather small, and none formed a second synapse.

Layer 6

The animal that provided particularly good anterograde labeling in layer 1 also had occasional collaterals in layer 6. These fine collaterals frequently branched as they passed through layer 6, and passed back and forth between the laminar boundaries. Bouton terminaux accounted for 25% of all boutons on labeled collaterals in layer 6.

We examined 28 boutons from layer 6 and found that 94% of the synapses were formed with spines (Fig. 5). Three of the target spines also formed a second synapse of a symmetric morphology.

Dendrites

Dendritic shafts represented only a small proportion (17%) of the synaptic targets observed in this study (Fig. 6). Typically, excitatory cells have spiny dendrites that contain few mitochondria and few synapses on the dendritic shaft. In contrast, the dendrites of inhibitory cells are spine-free or smooth, contain numerous mitochondria, and form many synapses on the shaft. They may also have widely variable diameter over their length. Dendrites showing these characteristics have also been demonstrated to be GABAergic (Somogyi et al., 1983; Peters and Saint Marie, 1984; Kisvárday et al., 1985; Ahmed et al., 1997). Here the majority of dendritic shafts were small in

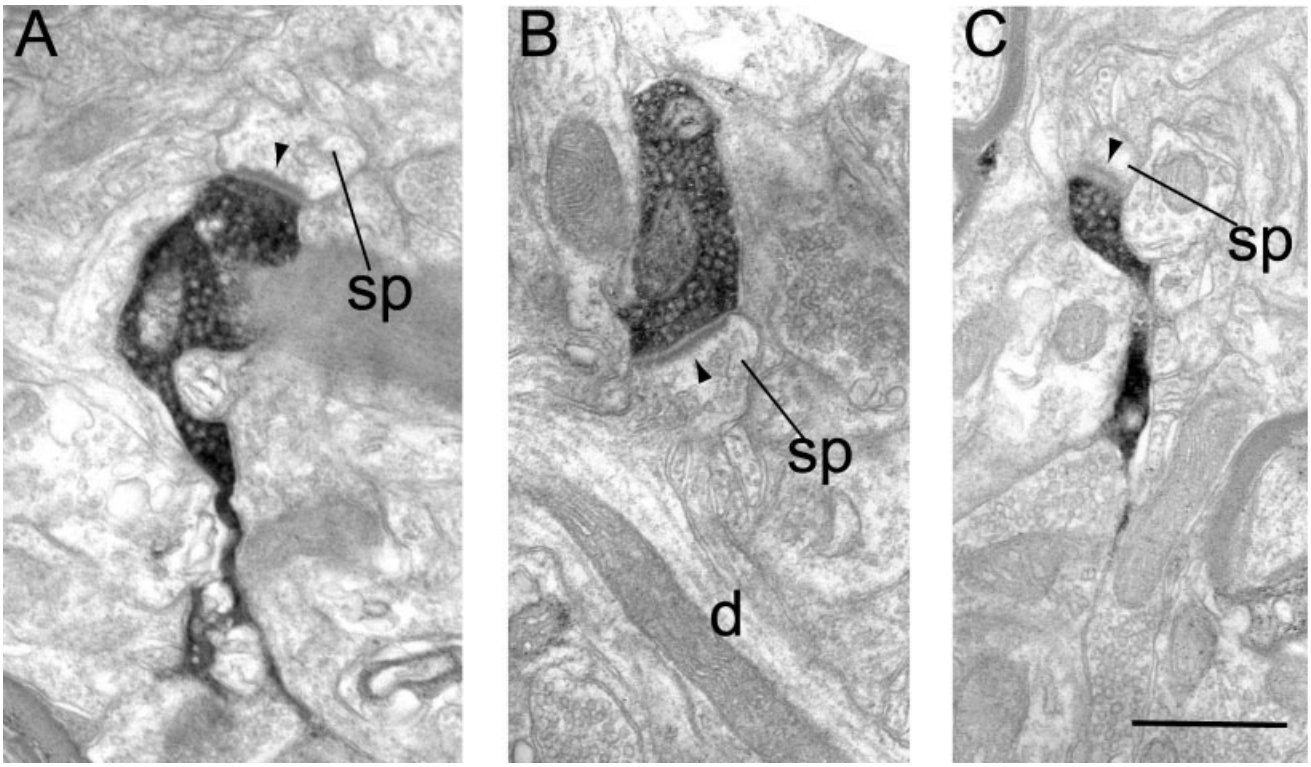

Fig. 5. Electron micrographs of BDA-labeled axons and boutons located in layer 6 of area V2. **A:** A labeled bouton forms an asymmetric synapse (solid arrowhead) with a spine (sp). **B:** A labeled bouton forms an asymmetric synapse with a spine that can be traced back to the parent dendrite (d). **C:** A small labeled bouton forms an asymmetric synapse (solid arrowhead) with a small spine (sp). Scale bar = 0.5 μm in C (applies to A–C).

diameter (~0.5 μm). In this study, serial section reconstruction was required to characterize neurons as smooth or spiny. On the basis of the established criteria, most of the target dendritic shafts (20/28 dendrites, 12.3% of all targets) originated from smooth, putative GABAergic neurons (e.g., Fig. 6A–D). The mean diameter of these dendrites at the position of the synapses was 0.58 μm.

Postsynaptic density

Reconstructing the boutons and their targets gave us the opportunity to view the complete postsynaptic density as a 2D or 3D structure. We have used this technique previously to obtain values for the surface area of synapses (Anderson et al., 1998; Anderson and Martin, 2002, 2005). By focusing on the postsynaptic specialization rather than the presynaptic membrane, we avoided detail being obscured by reaction endproduct in the bouton. We show a 2D projection of the postsynaptic densities in Figure 7. Comparisons between the distributions of the areas of synapses were confined to synapses made by spines due to the small numbers of dendritic synapses. There were few differences seen between those spinous synapses made by the different axons and the different laminae in which the samples were located (Fig. 8). The synapses of the clustered axon of layer 1 (axon 1; mean = 0.089 μm^2, SEM = 0.014) were not significantly different ($P = 0.196$, two-tailed t-test) from those of the random sample of layer 1 (mean, 0.117 μm^2, SEM = 0.015). Nor were the synapses of the unbranched axon (axon 2; mean, 0.126 μm^2; SEM = 0.022) significantly different from those of layer 1 ($P = 0.724$, two-tailed t-test). When comparing synapses from different laminae to those found in the random sample of layer 1, the layer 2/3 distributions overlapped considerably ($P = 0.36$, two-tailed t-test), while those of layer 6 (mean, 0.073 μm^2; SEM = 0.006) were significantly smaller ($P = 0.012$, two-tailed t-test).

There was no difference between the synapses of spines and dendrites when the data from all sources were pooled. The mean size of synapses with spines (mean, 0.1 μm^2; SEM = 0.006) was slightly larger than those of synapses with dendrites (mean, 0.08 μm^2; SEM = 0.009), although the difference was not significant ($P = 0.197$, two-tailed t-test).

The synapses of layer 1, layer 2/3, the clustered and the unbranched axons, all showed a longer tailed (skewed) distribution than the synapses of layer 6.

En face, the postsynaptic density could be a simple disc, or perforated, giving it a doughnut or horseshoe morphology. Figure 7 shows that the synapses with the more complex morphology are often formed with spines. A similar observation was made in the study of synapses made by V1 and V2 afferent boutons in area MT and V2 afferent boutons in area V3A (Anderson et al., 1998; Anderson and Martin, 2002, 2005).

Target types

The most frequently encountered targets of labeled boutons were spines. The major difference between the prin-

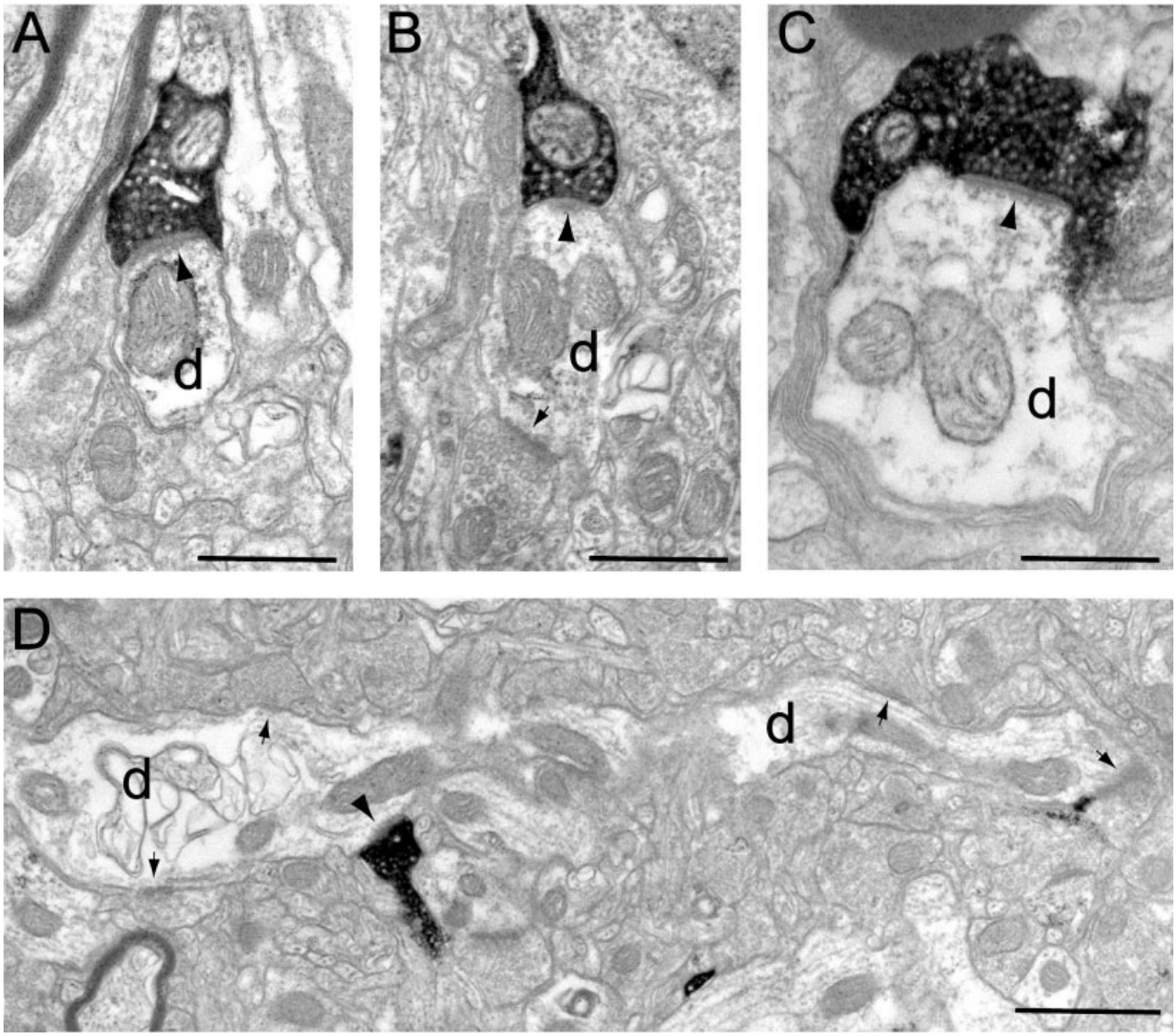

Fig. 6. Electron micrographs of labeled synaptic boutons forming synapses with dendrites containing numerous mitochondria and forming many synapses. These dendrites may also have a beaded morphology. These features are all characteristic of neurons that are GABAergic and have smooth dendrites. **A:** A labeled bouton forms an asymmetric synapse (solid arrowhead) with a small-caliber dendrite in layer 1. In subsequent sections the dendrite was seen to form asymmetric synapses with unidentified boutons. **B:** A small labeled bouton forms an asymmetric synapse (solid arrowhead) with a small-caliber dendrite (d) in layer 6. The dendrite forms an asymmetric synapse (small arrow) with an unidentified bouton. **C:** A large labeled bouton forms an asymmetric synapse (solid arrowhead) with a large-caliber dendrite (d) in layer 1. The dendrite contains many mitochondria and forms asymmetric synapses with other boutons when reconstructed from serial sections. **D:** A labeled bouton forms an asymmetric synapse (solid arrowhead) with a large-caliber dendrite in layer 1. The dendrite contains many mitochondria and forms numerous asymmetric synapses (small arrows) with unidentified boutons visible in the same section. Scale bars = 0.5 μm in A–C; 1 μm in D.

cipal laminae of innervation was in the proportion of spines to dendrites as targets, and for this reason we have shown all sources separately (random sampling and individual axons; Fig. 9). Taken together, the EM analysis shows that 80% of the labeled synapses in layer 1 were formed with spines and 20% were formed with dendritic shafts. In layer 6, 94% of the synapses were formed with spines and 6% with dendritic shafts (Fig. 9).

As indicated above (see Dendrites), smooth neurons provided the majority (69%) of the dendritic shaft targets in layer 1 and both of those in layer 6. The largest contributor to the putative non-GABAergic dendritic synapse was the random sample of layer 1, of which 42% (5/12) of dendrites were from spiny cells. The two axons in layer 1 both synapse only with the putative GABAergic type dendrite (4/4 and 3/3). In layer 2/3 almost all dendrites (6/7, 86%) were of the putative GABAergic type.

Serial reconstructions indicated that most boutons made only one synapse and only rarely more than two synapses (Fig. 10). On average, there were 1.1 synapses

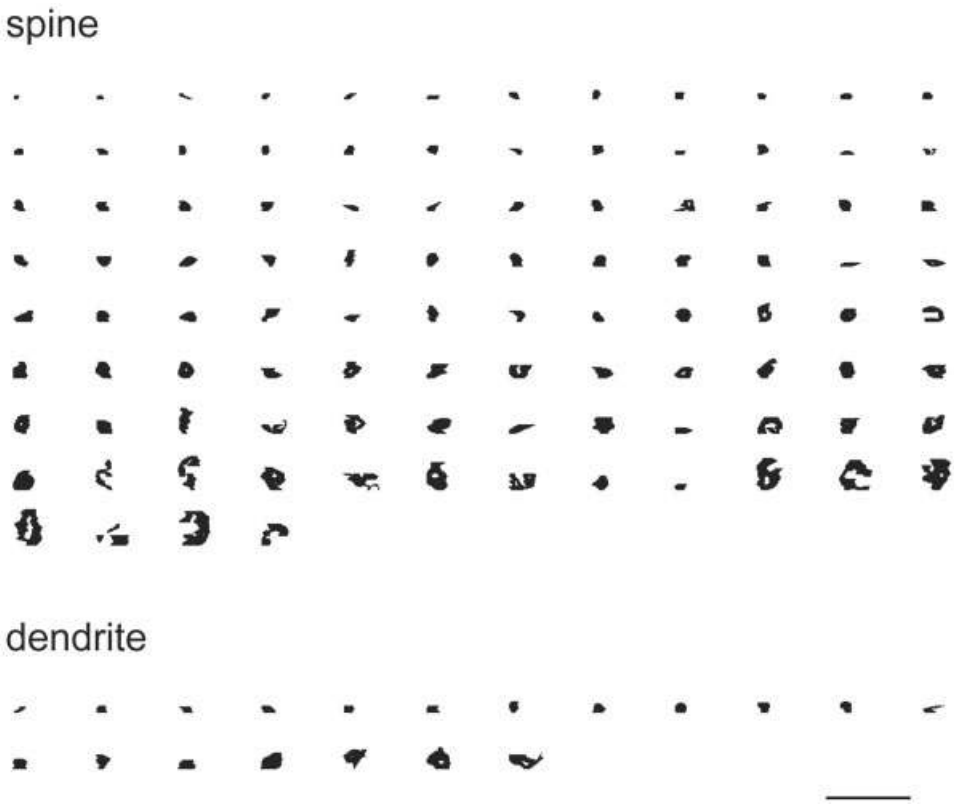

Fig. 7. Two-dimensional projection of the reconstructed postsynaptic densities found in layers 1, 2/3, and 6 on spines and dendrites postsynaptic to V4 labeled boutons in area V2. The densities are ordered by increasing surface area. Scale bar = 1 μm.

per labeled bouton. The sample with the highest synapse-to-bouton ratio was taken from layer 2/3, with 1.3 synapses per bouton, closely followed by the axon with the clustered terminals in layer 1, with 1.2 synapses per bouton. The random sample of 46 labeled boutons from layer 1 and 22 labeled boutons from the long, unbranched axon in layer 1 provided the lowest values in layer 1 of 1.05 and 1.04, respectively.

Synaptic density measurements

To estimate the relative proportion of synapses being contributed by V4 to V2, we made an unbiased stereological analysis of layer 1. We selected regions from within the densest areas of innervation for our analysis and applied the unbiased disector method (Sterio, 1984). We counted only those labeled synapses that disappeared in the "look-up" section when compared to a near adjacent "reference" section. Although the blocks of tissue used for reembedding were selected from the densest zones of innervation, the distribution of labeled synapses in any ultrathin section could vary greatly. From previous studies (Anderson and Martin, 2002) we know that if the disector region was selected using nonbiased features such as the edge of the tissue or a scratch on the block face, we counted no labeled synapses. If we selected the location of the disector by finding a labeled bouton and then sampling in the vicinity, we counted 2.2% (7 of 316) of disappearing labeled synapses. Larger patches of reconstructed tissue did not necessarily provide a higher proportion of disappearing labeled synapses. Some sample areas provided numerous boutons, but no disappearing synapses. We also noted more labeled axon profiles in this material than was seen in previous studies that looked at projections from lower to higher cortical areas terminating in layer 4.

DISCUSSION

The projection from V4 to V2 showed the classic features of a feedback projection (Kuypers et al., 1965; Pandya and Sanides, 1973; Tigges et al., 1974). We confirmed the observations of Rockland (1994, 1997; Rockland et al., 1994) that the major projection of individual axons was to layer 1, with additional sparse innervation of layers 2/3 and 6. In previous studies of feedforward projections we found patchy projections in layer 4 of the target area, despite large injections of tracers in the source area (Anderson et al., 1998; Anderson and Martin, 2002, 2005). By contrast, in the V4 projection to layer 1 of V2 the projections did not form patches. Although we found rare individual fibers that did form clustered terminals, most fibers traveled for millimeters through layer 1, presumably not aimlessly, but certainly being very discrete about what they were actually up to. This difference between the two modes of interareal connection, one punctate and patchy, the other diffuse, must reflect basic differences in their role in the circuit.

Our main interest here was in discovering whether there are qualitative or quantitative differences in the synaptic connections made by a feedback projection compared to other feedforward projections we have studied with the same methods. The projection neurons are typically glutamatergic pyramidal cells that connect mainly to other pyramidal cells. Our data were consistent with this pattern: 75% of the targets in layer 1 were spines and 94%

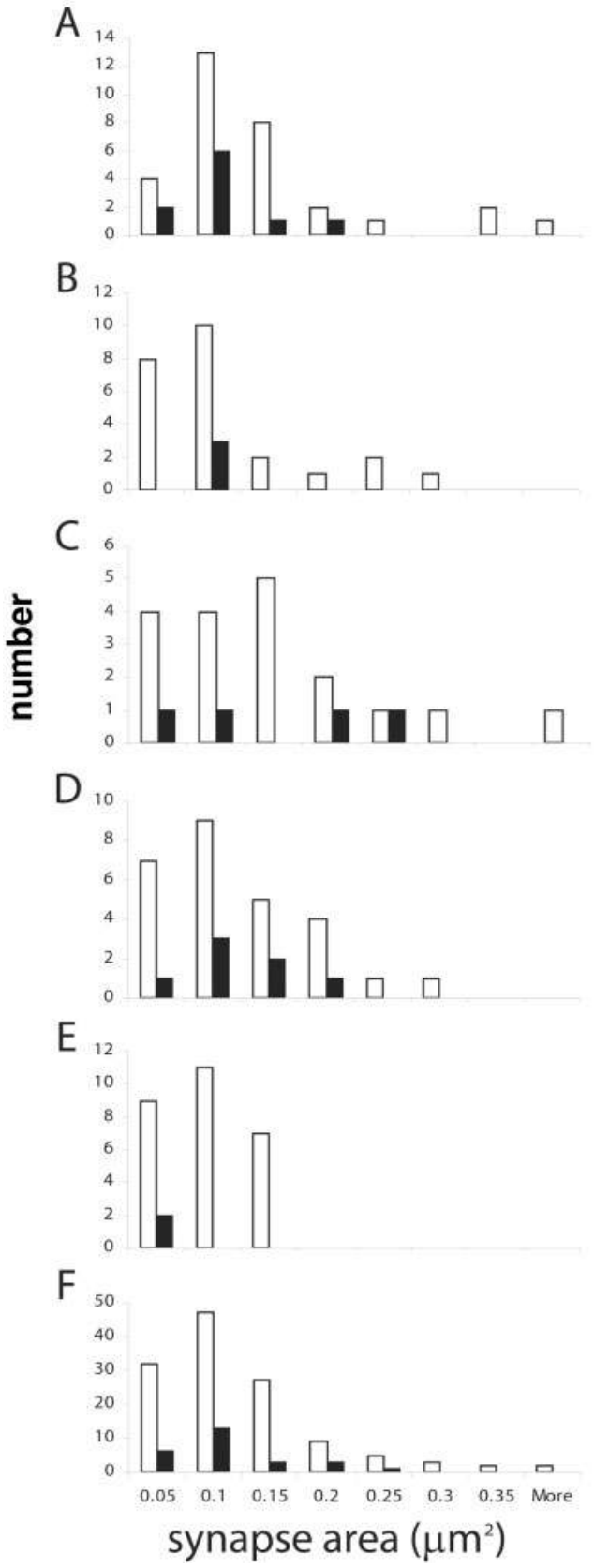

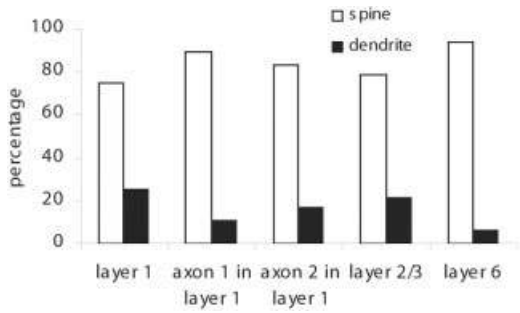

Fig. 9. Histogram of the synaptic targets of labeled V4 boutons in layers 1, 2/3, and 6 of area V2. For layer 1, n = 48; for clustered axon in layer 1, n = 27; for unbranched axon in layer 1, n = 23; for layer 2/3, n = 34; for layer 6, n = 31.

in layer 6 were spines. Rockland (1997) reported similar proportions for the feedback projection from V2 to V1 (82% spines, 18% dendritic shafts). These data indicate that pyramidal cells are the sole source and the major recipients of the intercortical connections.

As in the V2 to V1 projection studied by Rockland (1997), a minority of the targets of the V4 axons were dendritic shafts. We differentiated two types of dendrites, one of spiny, the other of smooth neurons, based on ultrastructural criteria examined over serial sections. Dendrites of smooth neurons formed 22/28 of the dendritic shafts that formed synapses with the V4 axons. This amounted to 12% of all targets. Taken together, these statistics lie well within the range of those we have compiled for feedforward projections using identical methods and criteria: the profile of synaptic targets for the V4 to V2 projection is broadly the same as that observed for the V1 to MT, the V2 to MT, and the V2 to V3A projections (Table 1; Anderson et al., 1998; Anderson and Martin, 2002, 2005).

The differences in the proportion of targets that were spines between the primary layer of innervation (layer 1; 73%) and the secondary layer of innervation (layer 6; 94%) was also a feature noted in two of the feedforward projections we studied, where layer 4 is the primary layer and layers 2/3 and 6 are the secondary layers. The synapses in layer 1 were formed mainly by en passant boutons, whereas 25% of the synapses in layer 6 were formed by bouton terminaux. In the projection from V2 to MT, 67% of the targets in layer 4 were spines, whereas in layer 2/3, 82% of the targets were spines. Similarly, in the feedforward projection from V2 to V3A, 76% of the layer 4 targets were spines, whereas in layer 2/3, 98% of the targets were spines. The major outlier was the projection from V1 to MT (Anderson et al., 1998), where spines formed only 54% of the targets in layers 4 and 6 and somata of smooth neurons formed a significant proportion (13%), with den-

Fig. 8. Histograms of the distribution of postsynaptic areas (μm^2) formed by labeled V4 boutons in layers 1, 2/3, and 6 of area V2. **A:** Unidentified labeled layer 1 synapses (n = 41). **B:** Synapses from axon with clustered terminals in layer 1 (Fig. 3) (n = 27). **C:** Synapses from unbranched axon in layer 1 (Fig. 4) (n = 22). **D:** Synapses from middle of layer 2/3 (Fig. 2) (n = 34). **E:** Synapses from layer 6 (Fig. 5) (n = 29). **F:** Pooled synapses of layers 1, 2/3, and 6 (n = 153).

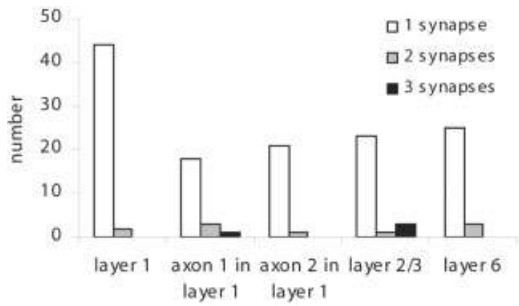

Fig. 10. Histogram of the number of synapses formed per labeled V4 bouton in layers 1, 2/3, and 6 of area V2.

dritic shafts of spiny neurons and smooth neurons making up the remainder. Also, no marked differences were seen between the principal layer (layer 4) and the secondary layer (layer 6) of termination in the proportion of innervated spines. However, in all other projections, V2 to MT, V2 to V3A, V4 to V2, there was a clear difference between the principal versus the secondary layer of innervation. A similar trend was observed by Johnson and Burkhalter (1996) for the feedforward projection from area 17 to the lateromedial area in the rat visual cortex. Here they noted that in layers 3 and 4, the primary layers of innervation, 87% of the targets were spines, whereas in the secondary layer, layer 1, 100% of the targets were spines. Since the dendritic shafts of smooth (presumed inhibitory) neurons form the majority of the targets that are not spines, it seems that a stronger inhibitory brake is required in the principal layer of termination than in the secondary layer or termination, where the density of synapses provided by the projection is in any event always extremely low. Similar trends have been noted in a combined ultrastructural and immunochemical study of the targets of the feedback and feedforward connections between area 17 and the lateromedial area in the rat cortex (Gonchar and Burkhalter, 2003).

The density, form, and size of the synaptic densities formed by the boutons were also studied. Here again, there were similarities with the feedforward pathways. If we chose EM sections with labeled synapses, we found that 2% of the asymmetric synapses in the densest part of the V4 to V2 projection were labeled. Using identical methods, the comparable percentages were 3% for the V1 to MT projection (Anderson et al., 1998), 4–6% for the V2 to MT projection (Anderson and Martin 2002), and 3.5–4.1% for the V2 to V3A projection (Anderson and Martin, 2005). In form, and in all interareal projections studied by us, the most complex shapes of the densities were always with spines. These synapses, which were also the largest, had perforated postsynaptic densities, which, when viewed en face, looked like horseshoes or doughnuts. The average size of the synapses on spines (~0.1 μm^2) was larger than those on dendritic shafts (0.08 μm^2) and the form of postsynaptic densities on dendritic shafts was always a simple disk. These same trends were seen in the feedforward projections cited above. For all projections we have studied, both feedforward and feedback, the average size of the spine synapses were within a close range of ~0.1–0.12 μm^2, while the synapses on dendritic shafts were ~0.07–0.09 μm^2.

TABLE 1. Putative GABAergic Targets of Interareal Connections[1]

		Projection			
		V1–V5	V2–V5	V2–V3A	V4–V2
%putative GABAergic targets	layer 1				**11**
	layer 2				18
	layer 3		8	0	
	layer 4	**18**	**15**	**10**	
	layer 6	14			6

[1]The proportion of putative GABAergic targets of three feedforward (V1 to V5, V2 to V5, V2 to V3A) (Anderson et al., 1998; Anderson and Martin, 2002, 2005) and one feedback projection (V4 to V2) in macaque cortex. The remainder of the targets were excitatory neurons. Principal layers of innervation are marked in bold. The V1 to V5 data included many somatic targets that formed multiple active zones with single boutons. These have been counted as single synapses for the purposes of this table.

From these comparisons, we conclude that the major differences between the feedback and feedforward projections are not to be found at the level of their synapses, possible differences in receptors notwithstanding. Both feedforward and feedback projections connect principally to spiny neurons, they both form synapses of similar size, and they both contribute only a few percent of the asymmetric synapses to the neuropil, even in their densest areas of innervation. Structurally, the major difference between the feedforward and feedback projections we have studied is thus the traditional one: the laminae they target. For the feedforward projections, the major targets are neurons in layer 4. For the feedback projection to layer 1, the distal tufts of the apical dendrites of pyramidal neurons form the major targets.

What differences in function are served by these differences in laminar termination of the feedforward and feedback projections, with their implicit differences in the position of their input on the dendritic trees of their target cells? At a biophysical level the differences between distal versus proximal synaptic inputs to pyramidal neurons have been the subject of intense debate. One recent view is that the location of the synapses does not matter (Magee and Cook, 2000), because in hippocampal pyramidal cells, at least, the excitatory synaptic conductance increases in proportion to the distance from the soma. The other view is that, as in real estate, location matters a great deal (Rall, 1967; Bernander et al., 1991; London and Segev, 2001). The principal argument for the importance of location is that if the neurons are embedded in an active network, the dendrites increase their electrotonic length due to the several-fold increase in membrane conductance produced by synaptic activity. More distal synapses are shunted by the increase in the conductance due to activation of synapses on more proximal dendrites. Since the apical tufts of the pyramidal cells are slender, inputs in layer 1 will be especially sensitive to the more proximal changes in conductance.

The receptive field size of feedforward and feedback pathways in V2 is different. In general, the receptive field sizes increase from V1, to V2, to V4 and MT (Van Essen and Zeki, 1978). Thus, for a given eccentricity the receptive fields of the neurons that feedback from V4 to V2 will be larger than the neurons to which they connect and much larger than the receptive fields of the V1 neurons that project to V2. Thus, an individual V2 neuron effectively "sees" a smaller piece of the visual field than its V4 neurons that provide the feedback inputs. This apparent paradox, that the V2 neurons have smaller receptive fields than their V4 inputs, suggests that the V4 inputs are not

driving the V2 neurons, but rather provide a modulation of the V2 activity.

What could be the role of this feedback from V4? One function that has been explored particularly in V2 and V4 of awake behaving monkeys is the role of attention. Attentional effects are seen throughout visual cortex and are manifest by an increased firing rate of neurons whose receptive fields lie in the attended part of the visual field. If two stimuli are placed within a single receptive field in V2, attention to one of the stimuli biases the responses of the neuron either up or down (Reynolds et al., 1999). The source of the biasing signal is unknown, but one candidate is, of course, the feedback from V4, where a similar interaction occurs (Reynolds et al., 1999). What seems clear from the anatomical data about the V4 to V2 feedback is that it does not seem well equipped to deliver fine-grained information to specific cells. At best, the feedback could provide a biasing signal that conveys simple information, delivered through a small excitatory input to many neurons.

LITERATURE CITED

Ahmed B, Anderson JC, Martin KAC, Nelson JC. 1997. Map of the synapses onto layer 4 basket cells of the primary visual cortex of the cat. J Comp Neurol 380:230–242.

Anderson JC, Martin KAC. 2002. Connection from cortical area V2 to MT in macaque monkey. J Comp Neurol 443:56–70.

Anderson JC, Martin KAC. 2005. Connection from cortical area V2 to V3A in macaque monkey. J Comp Neurol 488:320–330.

Anderson JC, Binzegger T, Martin KAC, Rockland KS. 1998. The connection from cortical area V1 to V5: a light and electron microscopic study. J Neurosci 18:10525–10540.

Bernander O, Douglas RJ, Martin KAC, Koch C. 1991. Synaptic background activity influences spatiotemporal integration in single pyramidal cells. Proc Natl Acad Sci U S A 88:11569–11573.

De Yoe EA, Van Essen DC. 1985. Segregation of efferent connections and receptive field properties in visual area V2 of the macaque. Nature 317:58–61.

Gonchar Y, Burkhalter A. 2003. Distinct GABAergic targets of feedforward and feedback connections between lower and higher areas of rat visual cortex. J Neurosci 23:10904–10912.

Kisvárday ZF, Martin KAC, Whitteridge D, Somogyi P. 1985. Synaptic connections of intracellularly filled clutch neurons, a type of small basket neuron in the visual cortex of the cat. J Comp Neurol 241:111–137.

Krubitzer LA, Kaas JH. 1989. Cortical integration of parallel pathways in the visual system of primates. Brain Res 478:161–165.

Kuypers HG, Szwarcbart MK, Mishkin M, Rosvold HE. 1965. Occipitotemporal corticocortical connections in the rhesus monkey. Exp Neurol 11:245–262.

Livingstone MS, Hubel DH. 1982. Thalamic inputs to cytochrome oxidase-rich regions in monkey visual cortex. Proc Natl Acad Sci U S A 79: 6098–6101.

Livingstone MS, Hubel DH. 1983. Specificity of cortico-cortical connections in monkey visual system. Nature 304:531–534.

London M, Segev I. 2001. Synaptic scaling in vitro and in vivo. Nat Neurosci 4:853–854.

Magee JC, Cook EP. 2000. Somatic EPSP amplitude is independent of synapse location in hippocampal pyramidal neurons. Nat Neurosci 3:895–903.

Munk M, Nowak L, Girard P, Chounlamountri N, Bullier J. 1995. Visual latencies in cytochrome oxidase bands of macaque area V2. Proc Natl Acad Sci U S A 92:988–992.

Pandya DN, Sanides F. 1973. Architectonic parcellation of the temporal operculum in rhesus monkey and its projection pattern. Z Anat Entwick 139:127–161.

Peters A, Saint Marie RL. 1984. Smooth and sparsely spinous nonpyramidal cells forming local axonal plexuses. In: Jones EG, Peters A, editors. Cerebral cortex, vol. 1. Cellular components of the cerebral cortex. New York: Plenum Press. p 419–445.

Peters A, Palay SL, Webster HDeF. 1991. The fine structure of the nervous system: neurons and their supporting cells, 3rd ed. Oxford: Oxford University Press.

Rall W. 1967. Distinguishing theoretical synaptic potentials computed for different soma-dendritic distributions of synaptic input. J Neurophysiol 30:1138–1168.

Reynolds JH, Chelazzi L, Desimone R. 1999. Competitive mechanisms subserve attention in macaque areas V2 and V4. J Neurosci 19:1736–1753.

Rockland KS. 1994. The organization of feedback connections from Area V2 (18) to V1 (17). In: Peters A, Rockland KS, editors. Cerebral cortex, vol. 10. Primary visual cortex in primates. New York: Plenum Press. p 261–299.

Rockland KS. 1997. Elements of cortical hierarchy revisited. In: Rockland KS, Kaas JH, Peters A, editors. Cerebral cortex, vol. 12. Extrastriate cortex in primates. New York: Plenum Press. p 243–293.

Rockland KS, Saleem KS, Tanaka K. 1994. Divergent feedback connections from areas V4 and TEO in the macaque. Vis Neurosci 11:579–600.

Shipp S, Zeki S. 1985. Segregation of pathways leading from area V2 to areas V4 and V5 of macaque monkey visual cortex. Nature 315:322–325.

Shipp S, Zeki S. 1989a. The organization of connections between area V5 and V1 in macaque monkey visual cortex. Eur J Neurosci 1:309–332.

Shipp S, Zeki S. 1989b. The organization of connections between areas V5 and V2 in macaque monkey visual cortex. Eur J Neurosci 1989 1:333–354.

Sincich LC, Horton JC. 2005. The circuitry of V1 and V2: integration of color, form and motion. Annu Rev Neurosci 28:303–326.

Somogyi P, Kisvárday Z F, Martin KAC, Whitteridge D. 1983. Synaptic connections of morphologically identified and physiologically characterised large basket cells in the striate cortex of cat. Neuroscience 10:261–294.

Sterio DC. 1984. The unbiased estimation of number and sizes of arbitrary particles using the disector. J Microsc 134:127–136.

Stettler DD, Das A, Bennett J, Gilbert CD. 2002. Lateral connectivity and contextual interactions in macaque primary visual cortex. Neuron 36: 739–750.

Suzuki W, Saleem KS, Tanaka K. 2000. Divergent backward projections from the anterior part of the inferotemporal cortex (area TE) in the macaque. J Comp Neurol 422:206–228.

Tigges J, Spatz WB, Tigges M. 1974. Efferent cortico-cortical fiber connections of area 18 in the squirrel monkey (Saimiri). J Comp Neurol 158:219–235.

Van Essen DC, Zeki SM. 1978. The topographic organization of rhesus monkey prestriate cortex. J Physiol 277:193–226.

Zeki S. 1969. Representation of central visual fields in prestriate cortex of monkey. Brain Res 14:271–291.

Zeki S. 1973. Colour coding in rhesus monkey prestriate cortex. Brain Res 53:422–427.

Zeki S, Shipp S. 1989. Modular connections between areas V2 and V4 of macaque monkey visual cortex. Eur J Neurosci 1:494–506.